Highlights from the PHENIX experiment - Part 1

S. V. Greene[a] (for the PHENIX* Collaboration)

[a]Department of Physics and Astronomy, Vanderbilt University,
Box 1807 Station B, Nashville, Tennessee, USA

This paper is the first of a two-part series on recent highlights from the PHENIX experiment at the Relativistic Heavy Ion Collider at Brookhaven National Laboratory. A summary of conclusions reached after the first four years of RHIC running is presented. The focus of the paper is on new experimental results related to thermalization, hadronization, and energy loss mechanisms.

1. THE FIRST EPOCH OF RHIC

The first epoch of RHIC running and data analysis culminated in the publication of summary papers by each of the four experiments: PHENIX, STAR, BRAHMS, and PHOBOS [1–4]. These "White papers" collected and synthesized results from data spanning the first three years of RHIC running. PHENIX drew several significant conclusions from examining these measurements. At the most fundamental level, the energy densities formed in Au+Au collisions at $\sqrt{s_{NN}} = 200$ GeV/c are found to be 15 GeV/fm^3, estimated using the Bjorken formalism with dN/dy as measured by PHENIX [1,5]. This is considerably greater than the 1 GeV/fm^3 predicted by lattice QCD as the energy density needed to form a deconfined state.

One of the most significant conclusions is the observation that jets produced from hard scattering of quarks are suppressed in central Au+Au collisions [6–8]. The suppression is quantified by the nucear modification factor R_{AA}, the ratio of the measured particle spectra to that expected from scaling the spectra from p+p collisions to reflect the number of p+p interactions in Au+Au collisions. The suppression is flat as a function of transverse momentum for $p_t < 10$ GeV/c. Complementary measurements from d+Au collisions show no such suppression [9]. Taken together, these observations lead to the conclusion that the suppression results from the state of the system after the collision rather than to effects arising from the initial nuclear state.

Another important observation from the first RHIC epoch is that strong elliptic flow is seen in central Au+Au collisions at $\sqrt{s_{NN}} = 200$ GeV/c [10]. This flow is measured by v_2, the most significant coefficient in the Fourier expansion of the azimuthal anisotropy. The scaling of v_2 with eccentricity indicates that a high degree of collectivity is evident even in the early stages of the collision. This observation is interpreted as evidence for very early thermalization. These data can be described by ideal hydrodynamic models, in

*For the full list of PHENIX authors and acknowledgments, see appendix 'Collaborations' of this volume.

which the properties of the matter produced after the collision are consistent with those of a liquid ([1]).

The early running period of RHIC has clearly increased our understanding of the system produced at extreme temperatures and densities. It has also focused the objects of our inquiry for future experiments at RHIC. The key predictions that derive from the properties of the quark-gluon plasma need to be refined and tested using data from Run-4 and beyond. Areas that need further study include R_{AA} at very high p_T, the energy loss of particles containing heavy quarks, the source of the anomalous proton/pion ratio, and chiral symmetry restoration.

This paper takes as a starting point the conclusions of the PHENIX white paper and charts the progress in the approximately one year since its completion. The focus is on global variables, spectra, and flow. The companion paper in this volume, "Highlights from the PHENIX experiment - Part 2" (see Büsching, these Proceedings) reports on the physics of thermal radiation, the fate of the J/ψ, and the modification of jets in the medium.

2. THE PHENIX DETECTOR

The PHENIX detector has been extensively described elsewhere [11] and so this paper includes only a brief overview and a description of recent upgrades. PHENIX comprises a central spectrometer with two arms that identify hadrons, electrons, and photons and a muon spectrometer with two arms along the forward and backward beam directions. Upgrades to the data acquisition and trigger systems include new Level-1 triggers for muon and electron measurents, improved Level-2 filtering, and an increased DAQ rate. In addition, a system for online calibrations allows for much faster analysis as evidenced by the availability of results from Cu+Cu collisions only a few months after the end of Run-5. Finally, a new aerogel counter has extended the p_T reach of the central spectrometer and the resistive plate chambers that will measure time-of-flight in conjunction with the aerogel counter were successfully tested in Run-5.

3. THERMALIZATION

The collective behavior of the system as it evolves after the collision reflects the degree to which the partons have thermalized. The standard measure of this collectivity is anisotropic flow where the initial spatial anisotropy of the collision system is converted into momentum anisotropy. The efficiency of the conversion depends on the properties of the medium. The anisotropic flow is commonly quantified by v_2, the second coefficient in a Fourier expansion of the azimuthal distribution of the emitted particles. The later a system thermalizes, the less the spatial anisotropy develops the smaller the v_2. Conversely, a larger v_2 implies early thermalization.

PHENIX has measured v_2 for a number of different particle species of differing mass, including pions, ϕ's, kaons, protons, and deuterons (see Masui, Winter, and Pal, these Proceedings). We can also extract a heavy flavor signal by measuring the number of electrons in excess of the large photonic electron signal (see Butsyk, these Proceedings). The observed v_2 of these non-photonic electrons gives a measurement of the thermalization of heavy flavor produced in semileptonic decays such as $D^0 \rightarrow K^- + e^+ + \nu_e$. Figure 1

shows a compilation of v_2 as a function of p_T for minimum bias Au+Au collisions at $\sqrt{s_{NN}}$ = 200 GeV/c. All particle species show significant v_2, suggesting that even the heaviest particles such as the ϕ and the deuteron thermalize early in the development of the system after collision. Although the experimental uncertainties are large for the open charm signal, the result does suggest that particles containing charmed quarks exhibit early thermal behavior as well.

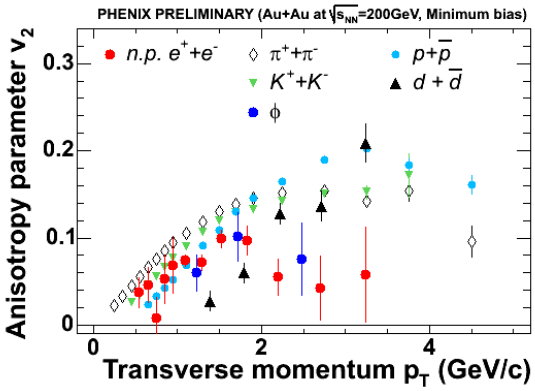

Figure 1. The anisotropy parameter v_2 as a function of p_T for minimum bias Au+Au collisions at $\sqrt{s_{NN}}$ = 200 GeV/c. Results are shown for non-photonic electrons (red circles), charged pions (open diamonds), charged kaons (green triangles), ϕ mesons (blue circles), protons (cyan circles), and deuterons (black triangles).

It is interesting to probe deeper into the behavior of the process of thermalization by raising the question as to whether azimuthal flow develops at the partonic level. Figure 2 shows the same data described above, but with the p_T and v_2 per number of quarks plotted on the horizontal and vertical axes. The results show that parton flow is observed, suggesting that a thermalized system of partons is indeed produced.

The first data for Cu+Cu collisions at $\sqrt{s_{NN}}$ = 200 GeV/c were taken during Run-5, the RHIC data-taking period that ended a few months before the Quark Matter '05 conference. Figure 3 shows preliminary results for charged hadron v_2 vs p_T comparing minimum bias Cu+Cu and Au+Au collisions. A significant v_2 is clearly seen in the lighter collision system as well as the heavier, but systematic study is needed to give a detailed account of the implications of the new Cu+Cu results.

4. HADRONIZATION

Data discussed in the previous section show that v_2 obeys simple valence quark scaling, indicating that thermalization occurs at the partonic level. This observation implies that the scaling arises from the coalescence of quarks. Here the details of the hadronization process become significant. The data have led us to ask several important questions about the transition from a partonic to a hadronic system. For instance, we observe a large

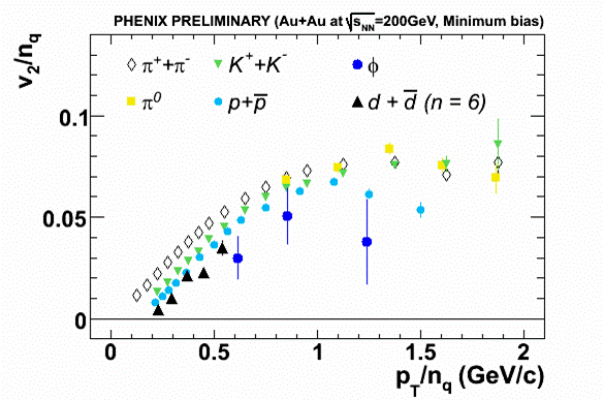

Figure 2. The anisotropy parameter v_2 per number of quarks vs. p_T per number of quarks for minimum bias Au+Au collisions at $\sqrt{s_{NN}} = 200$ GeV/c. Results are shown for charged pions (open diamonds), π^0's (yellow squares), charged kaons (green triangles), protons (cyan circles), ϕ mesons (blue circles), and deuterons (black triangles).

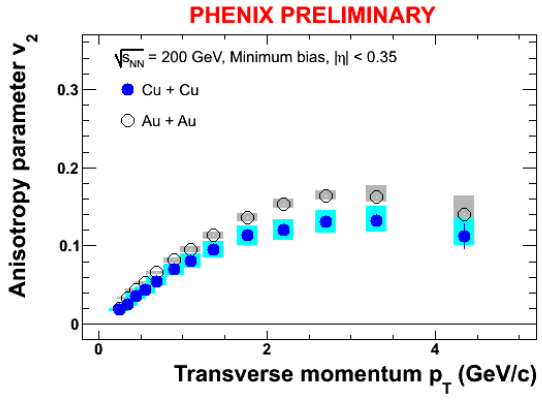

Figure 3. The anisotropy parameter v_2 as a function of p_T for minimum bias collisions at $\sqrt{s_{NN}} = 200$ GeV/c and $|\eta| < 0.35$. Results are shown for charged hadrons produced in collisions between Au+Au (open circles) and Cu+Cu (blue circles).

proton to pion ratio at higher p_T. Having determined that final-state interactions lead to the suppression of pions, it is not understood why the protons are less suppressed than the pions. The in-medium energy loss of a parton propagating through the system followed by fragmentation into hadrons should affect the production of all hadrons similarly. Some probable pieces of the baryon puzzle are flow, recombination, and parton energy loss. This section presents recent PHENIX results that address these issues.

The recombination model indicates that at low p_T, the quarks coalesce into hadrons locally in space and time [12,13]. If the quark and antiquark spectra are thermal, the p_T spectrum for hadrons is shifted to higher values of p_T. This picture is in contrast to expectations for spectra described by fragmentation models, where the hadronization process starts with a single fast parton and subsequent energy loss should have a similar effect on both pions and protons [14]. Thus recombination could account for the large p/π ratio at higher p_T.

Figure 4 shows the ratio of antiprotons to π^- as a function of p_T for Au+Au and Cu+Cu collisions at $\sqrt{s_{NN}} = 200$ GeV/c for two centrality bins (see Konno, these Proceedings). Figure 5 shows the same ratio as a function of the number of participants, $N_{\rm part}$ but for particles with $p_t = 2$ GeV/c. The Cu+Cu results show that the scaling of $\bar{p}/\pi^-$ with $N_{\rm part}$ is similar to that previously seen in Au+Au collisions. Note that these results are not corrected for feed-down from higher resonance decay. The observed scaling of the baryon to meson ratio is not specific to Au+Au, but rather is smooth as a function of the number of participants.

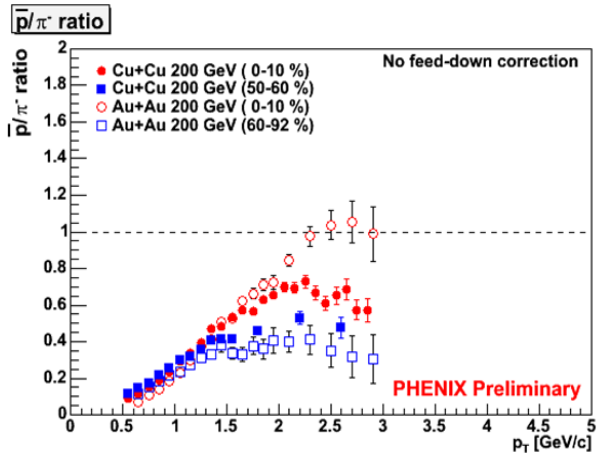

Figure 4. The ratio of $\bar{p}/\pi^-$ as a function of p_T for central (0-10%; solid red circles) and more peripheral (50-60%; solid blue squares) Cu+Cu collisions and central (0-10%; open red circles) and more peripheral (60-92%; open blue squares) Au+Au collisions at $\sqrt{s_{NN}} = 200$ GeV/c.

A possible path towards a solution to the baryon puzzle is to observe how the suppression varies with particle properties. The pion, a meson, has a smaller mass than the

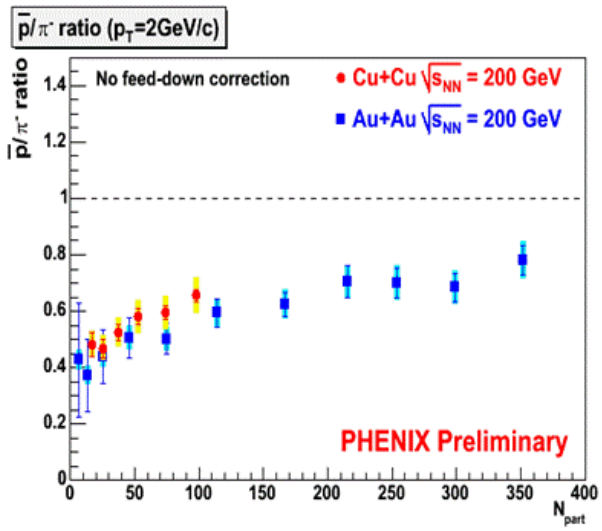

Figure 5. The ratio of $\bar{p}/\pi^-$ as a function of $N_{\rm part}$ for central (0-10%; solid red circles) Cu+Cu collisions and central (0-10%; blue circles)) Au+Au collisions at $\sqrt{s_{NN}}$ = 200 GeV/c.

proton, a baryon. The ϕ makes a good probe of these differences since it is a meson like the pion but has a mass similar to that of a proton. PHENIX has measured the nuclear modification factor, $R_{\rm AA}$, as a function of p_T for the decay channel $\phi \rightarrow K^+K^-$. Figure 6 shows $R_{\rm AA}$ vs p_T in Au+Au collisions at $\sqrt{s_{NN}} = 200$ GeV/c for ϕ, protons, and π^0 (see Pal, these proceedings). The pion spectra have recently been extended to high p_T using the aerogel detector upgrade. The ϕ follows the same trend as the π rather than the proton, suggesting that meson-baryon differences rather than mass effects are responsible for the marked difference in the nuclear modification factor.

5. R_{AA} AT HIGH p_T

PHENIX has extended the reach of its previous measurements of the nuclear modification factor R_{AA}, to significantly higher p_T. Figure 7 shows the π^0 R_{AA} as a function of p_T in $\sqrt{s_{NN}} = 200$ GeV/c Au+Au collisions for the 10% most central events (see Winter, these proceedings). R_{AA} appears flat out to 20 GeV/c. Models with parton energy loss can reproduce the nearly flat R_{AA} for $3 < p_t < 20$ GeV/c [14]. However, PHENIX measurements of π v_2 indicate that at intermediate p_T additional physics beyond energy loss is needed to describe the data. Thus, our understanding of the physics in the intermediate p_T region is incomplete.

In Run-5, PHENIX has measured R_{AA} for π^0's in Cu+Cu collisions at $\sqrt{s_{NN}} = 200$ GeV/c (see Shimomura, these proceedings). Figure 8 shows R_{AA} vs. the number of participants, $N_{\rm part}$, for the hard scattering region $p_t > 7$ GeV/c. The centrality dependence of the suppression in Cu+Cu shows a roughly similar scaling behavior as in Au+Au.

PHENIX has also measured the nuclear modification factor for electrons produced from

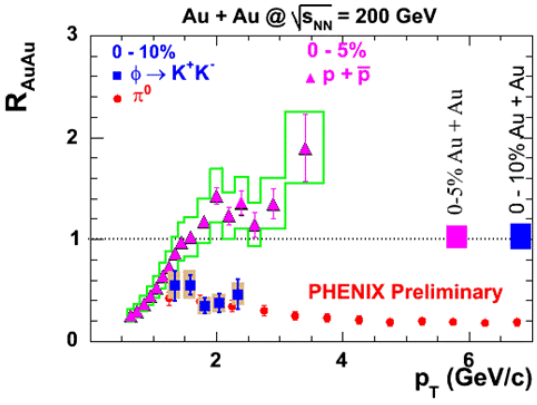

Figure 6. The nuclear modification factor $R_{\rm AA}$ as a function of p_T for $\sqrt{s_{NN}} = 200$ GeV/c Au+Au collisions. Results are shown for $\phi \rightarrow K^+K^-$ (0-10% central; blue squares), π^0's (0-10% central; red circles), and protons and antiprotons (0-5% central; magenta triangles).

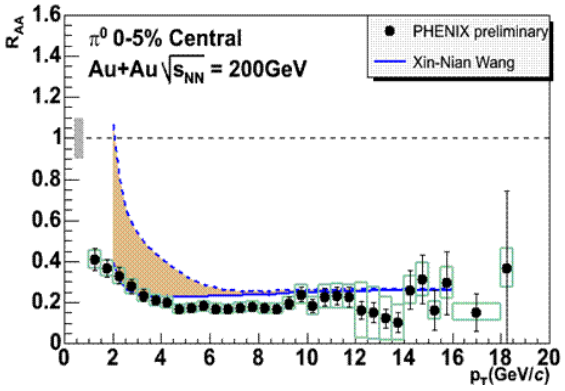

Figure 7. The nuclear modification factor $R_{\rm AA}$ as a function of p_T for central $\sqrt{s_{NN}} = 200$ GeV/c Au+Au collisions. Results are shown for π^0's. The calculation is from [14].

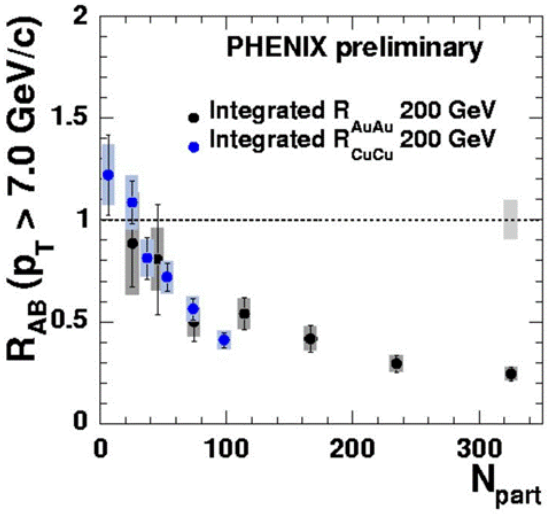

Figure 8. The nuclear modification factor $R_{\rm AA}$ for π^0's as a function of the number of participants ($N_{\rm part}$) for central $\sqrt{s_{NN}}$ = 200 GeV/c Cu+Cu (blue circles) and Au+Au (black circles) collisions. Results are integrated over $p_t > 7$ GeV/c.

semileptonic decays of heavy quarks. The spectra of electrons from decays of particles having open charm or bottom quarks can be separated from copious sources of electrons such as photon conversions and Dalitz decays. PHENIX uses two distinct methods for determing the contribution from photonic sources. First, a cocktail of known photonic sources is generated and subsequently subtracted from the total electron spectrum. Second, the photonic contribution is measured directly by putting additional material of known radiation length into the PHENIX detector (see Butsyk, these Proceedings).

The results are shown in Figure 9, which shows $R_{\rm AA}$ vs. p_T for the 10% most central collisions for $\sqrt{s_{NN}}$ = 200 GeV/c Au+Au collisions. Strong suppression is observed for $p_t > 1$ GeV/c. Theoretical calculations for the final state energy loss of heavy flavor are also shown. The curves from Armesto, et al. [15] include three values of the transport coefficient $\hat{q}$. The best agreement is found using an extremely large value for $\hat{q}$ of 14 GeV^2/fm.

An indirect measure of azimuthal flow of heavy quarks can be made by determining the v_2 of semileptonic electrons. Simulations and converter measurements of v_2 of photonic electrons can be used to disentangle this contribution from electrons resulting from semileptonic decays of particles with open heavy quark content. Preliminary results shown in Figure 10 suggest that v_2 is nonzero for these nonphotonic electrons. The v_2 is reduced in strength for $p_t > 2$ GeV/c. The nonphotonic electrons probably come from a mixture of particles with open charm and bottom. In order to understand the development of v_2 in heavy quark systems, it will be necessary to understand the contribution of bottom v_2 to the measurement, since the heavier quark is expected to have a lower v_2 which could account for the drop in v_2 at $p_t > 2$ GeV/c.

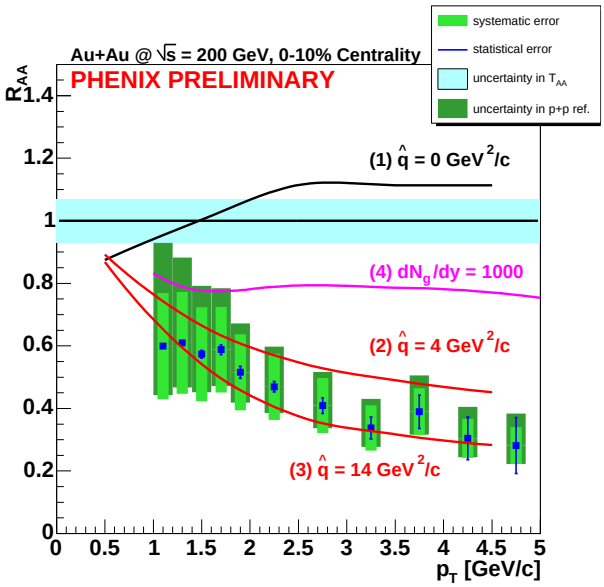

Figure 9. The nuclear modification factor $R_{\rm AA}$ vs. p_T for electrons from semileptonic heavy flavor decays for the 10% most central collisions for $\sqrt{s_{NN}} = 200$ GeV/c Au+Au collisions. The calculations of final state energy loss using different values of the transport coefficient $\hat{q}$ are from [15] and [16].

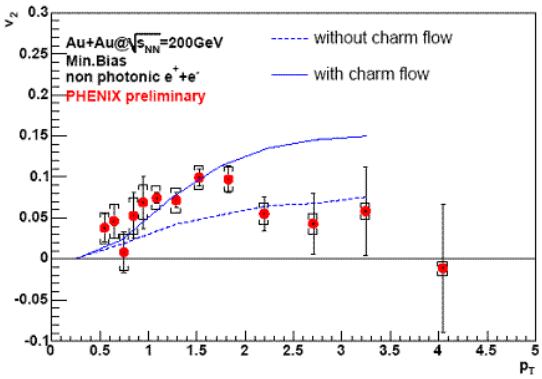

Figure 10. The anisotropy parameter v_2 for electrons from semileptonic heavy flavor decays as a function of p_T for minimum bias collisions at $\sqrt{s_{NN}} = 200$ GeV/c. Calculations are from Greco, Ko, and Rapp [17].

6. CONCLUSIONS

PHENIX has observed significant v_2 for particles as heavy as ϕ-mesons, suggesting that significant thermalization occurs early in the collision. We see a smooth dependence on $N_{\rm part}$ of the baryon-meson ratio in Cu+Cu and Au+Au collisions at $\sqrt{s_{NN}} = 200$ GeV/c. At high p_T, v_2 measurements indicates that pQCD with energy loss dominates above 7 GeV/c while below this energy, additional physics is needed to describe the data. $R_{\rm AA}$ at high p_T appears to be flat for p_t up to 20 GeV/c. Finally, suppression in Cu+Cu mid-central collisions is similar to peripheral Au+Au collisions.

In addition, PHENIX has measured a large nuclear modification factor for electrons from semileptonic heavy flavor decays in central Au+Au collisions. The v_2 of electrons from heavy flavor decays is clearly nonzero for $p_t < 2$ GeV/c and decreases thereafter, although measurement errors in this region are large.

Experimental results from RHIC continue to present puzzles along with an increased understanding of the fundamental processes of thermalization, hadronization, and energy loss. PHENIX has accomplished the initial goal of exploring the nature of matter under extremely high temperatures and densities. The further challenge of characterizing this matter and probing the detailed properties is the goal for the next RHIC epoch.

REFERENCES

1. K. Adcox Nucl.Phys.A **757** (2005) 184.
2. J. Adams *et al.*, Nucl.Phys.A **757** (2005) 102.
3. I. Arsene *et al.*, Nucl.Phys.A **757** (2005) 1.
4. B. B. Back *et al.*, Nucl.Phys.A **757** (2005) 28.
5. S. S. Adler, *et al.*, Phys. Rev. C **71**(2005) 034908.
6. K. Adcox, *et al.*, Phys. Lett. B **561** (2003) 82.
7. S. S. Adler, *et al.*, Phys. Rev. Lett. **91** (2003) 072301.
8. S. S. Adler, *et al.*, Phys. Rev. C **69** (2004) 034910.
9. S. S. Adler, *et al.*, Phys. Rev. Lett. **91**(2003) 072303.
10. S. S. Adler, *et al.*, Phys. Rev. Lett. **91** (2003) 182301.
11. K. Adcox, *et al.*, NIM A **499** (2003) 345.
12. R. J. Fries, B. Muller, C. Nonaka, S. A. Bass, Phys. Rev. Lett. **90** (2003) 202303.
13. R. J. Fries, B. Muller, C. Nonaka, S. A. Bass, Phys. Rev. C **68** (2003) 044902.
14. X.-N. Wang, Phys. Lett. B 595 (2004) 165.
15. N. Armesto, S. Dainese, C. Salgado, and U. Wiedemann, Phys. Rev. D **71**, (2005) 054027.
16. M. Djordjevic, M. Gyulassy, R. Vogt, S. Wicks, nucl-th/0507019
17. V. Greco, C. M. Ko, R. Rapp, Phys.Lett.B 595 (2004) 202.